Electronic Supplementary Material (ESI) for Journal of Materials Chemistry A.
This journal is © The Royal Society of Chemistry 2023

Supporting information

Seed mediated formation of multiphase zero-valent Sb nanoparticles as alloying-type anodes for sodium-ion batteries with high capacity and ultra-long durability

Weixu Wang,[a] Yongjie Wang,[b] Zhongqing Jiang,[c] Binglu Deng[d] and Zhong-Jie Jiang*[a]

[a] Guangzhou Key Laboratory for Surface Chemistry of Energy Materials, Guangdong Engineering and Technology Research Center for Surface Chemistry of Energy Materials, College of Environment and Energy, South China University of Technology, Guangzhou 510006, P. R. China. E-mail: eszjiang@scut.edu.cn and zhongjiejiang1978@hotmail.com.

[b] Guangdong Provincial Key Laboratory of Semiconductor Optoelectronic Materials and Intelligent Photonic Systems, Harbin Institute of Technology, Shenzhen 518055, P. R. China.

[c] Key Laboratory of Optical Field Manipulation of Zhejiang Province, Department of Physics, Zhejiang Sci-Tech University, Hangzhou 310018, P. R. China.

[d] School of Materials Science and Hydrogen Energy, Foshan University, Foshan 528000, P. R. China.

Experimental section

Chemicals

Multi-walled carbon nanotubes (CNTs) was obtained from Shenzhen Nanotech Port Co., Ltd. Antimony (III) acetate ($Sb(Ac)_3$, ≥97.0%), ethylene glycol (≥98.0%), carboxymethyl cellulose sodium (≥99.0%) and cobalt acetate ($Co(Ac)_2 \cdot 4H_2O$, ≥98.0%) were purchased from Macklin. N, N-Dimethylformamide (DMF) (C_3H_7NO, ≥99.5%), and absolute ethanol (EtOH, ≥99.7%) were bought from Tianjin Damao Chemical reagents Co., Ltd. Nitric acid (HNO_3, 65.0~68.0%) and sulfuric acid (H_2SO_4, 95.0~98.0%) were bought from Guangzhou Chemical reagents Co., Ltd. All the chemicals were utilized as received. De-ionized water (with resistance of 18.2 MΩ cm^{-1}) was utilized for all the experiments.

Preparation of CoSb/CNTs

The CNTs used in this work was functionalized by the acid treatment using the method reported previously.[1] 60.0 mg of the acid treated CNTs were then redispersed in 24.0 mL DMF under ultrasonication. 10.0 mL of 0.05 mol L^{-1} $Sb(Ac)_3$ in ethanol/ethylene glycol ($V_{ethanol}$:V_{glycol} =3.0:1.0) and 6.0 mL 0.05 mol L^{-1} $Co(Ac)_2$ in ethanol/ethylene glycol ($V_{ethanol}$:V_{glycol} =3.0:1.0) were then successively added. The reaction mixture was then solvothermally heated at 180 °C for 12 h. The obtained CoSb/CNTs was then washed with water and ethanol by centrifugation and finally dried at an oven at 60 °C for 12 h.

Preparation of NC@CoSb/CNTs

For the synthesis of NC@CoSb/CNTs, 40.0 mg of the CoSb/CNTs synthesized above were redispersed in 40.0 mL water under ultrasonication. 10.0 mL of 0.46 mol L^{-1} $FeCl_3$ and 0.1 mL of pyrrole was then added. The reaction was last for 2 h. This was followed by the addition of another 0.1 mL of pyrrole. After another 2 h of the reaction, the obtained PPY@CoSb/CNTs was collected by centrifugation, thoroughly washed with ethanol for >3 times, and finally dried in an oven at 60 °C. The obtained PPY@CoSb/CNTs was then loaded onto the tube furnish and calcined at 300, 350, 400, and 450 °C, respectively, under the N_2 atmosphere for 2 h. The obtained products were named as the NC@CoSb/CNTs-X with X representing the calcination temperature. To investigate the influence of the Co content on the electrochemical properties of the NC@CoSb/CNTs-400, the PPY@CoSb/CNTs were prepared from the CoSb/CNTs synthesized using 0, 2.0 and 10.0 mL of $Co(Ac)_2$ while keeping other parameters constant and then calcined at 400 °C. For comparison, the NC@Co/CNTs-400 were also prepared using the same procedure albeit in the absence of $Sb(Ac)_3$.

Characterization

A Bruker D8 ADVANCE (Germany) diffractometer with Cu Kα radiation (λ = 1.5406 Å) was employed to collect X-ray diffraction (XRD) patterns. SEM and TEM images were obtained on field emission scanning electron microscopy (S-4800, Japan) at 5.0 kV and transmission electron microscope (JEOL-JEM 2100 F, Japan) at 200 KV, respectively. The thermogravimetric analysis (TGA) was carried out on NETZSCH

STA 449F5 at a ramp of 10.0 °C min^{-1} under air. A Thermo Scientific K-Alpha instrument with an Al Kα source (hν = 1486.6eV) was utilized to obtain X-ray photoelectron spectroscopic (XPS) spectra. All the peaks are calibrated with C 1s at 284.8 eV.

Electrochemical measurement

The working electrode was fabricated by drop-casting the slurry of the active material, carbon black, and carboxymethyl cellulose sodium with a mass ratio of 7:2:1 in water onto the Cu foil and vacuum drying at 60 °C for 12 h. The electrode was then cut into disks with a diameter of ~ 13.0 mm. The mass loading of the active material was controlled to be ~ 1.0 mg cm^{-2}. The CR2025 coin cells were used for electrochemical tests, which were assembled in an argon-filled glovebox. The sodium foil and the glass fiber (Whatman GF/D) were utilized as the counter electrode and separator, respectively; 1.0 mol L^{-1} $\mathrm{NaClO_4}$ in the EC/DEC solution (V_{EC}:V_{EDC}=1.0:1.0) containing 5.0 % FEC as the electrolyte. A Land CT2001A battery test system (Wuhan Land Electronics Co. Ltd.) was employed to test the performance of the samples at room temperature (25 °C). The Na^{+} diffusion coefficients were estimated by the Galvanostatic intermittent titration technique (GITT). Before the GITT testing, the cell was discharged/charged at 0.1 A g^{-1} for 10 min. This was followed by keeping it at the open circuit voltage for 90 min to facilitate the relaxation back to equilibrium. The procedure was repeated until the discharge/charge voltage reached to 0.01/3.0 V. Cyclic voltammograms (CVs) were obtained on an electrochemical platform CHI660E (Chen Hua, Shanghai, China) with the scanning rates in the range of 0.1-1.6 mV s^{-1} within the voltage window of 0.01–3.0 V vs. Na^{+}/Na.

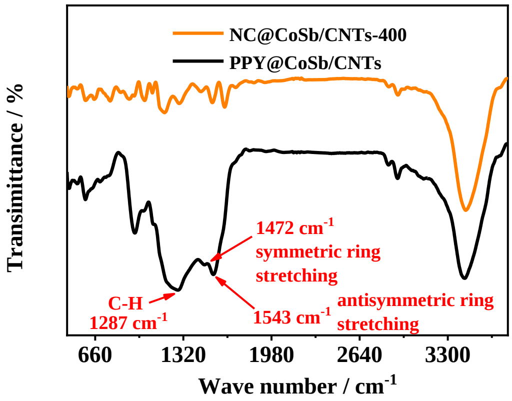

Figure S1. FTIR spectra of PPY@CoSb/CNTs and NC@CoSb/CNTs-400.

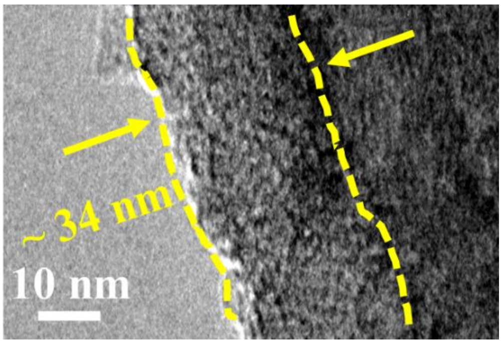

Figure S2. TEM image of PPY@CoSb/CNTs.

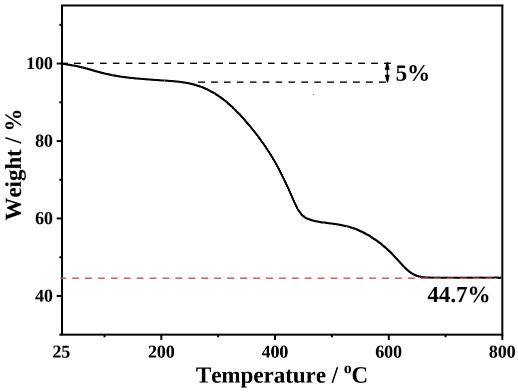

Figure S3. TGA curve of NC@CoSb/CNTs-400.

The ICP-OES results show that the atomic ratio of Co:Sb in the NC@CoSb/CNTs-400 is 1.00:4.60 (consistent with XPS result, 1.00:4.58), indicating an atomic ratio of Sb in the CoSb is 0.82. Since the final oxidation product of Sb after the TGA is Sb_2O_4,[2] the content of Sb in the NC@CoSb/CNTs-400 can be estimated based on the TGA result:

$$Sb\ content\ (\mathrm{wt\%}) = \frac{2\times M_{Sb}}{M_{Sb_2O_4}} \times \frac{0.82\times M_{Sb_2O_4}}{0.82\times M_{Sb_2O_4}+0.18\times M_{Co_2O_3}} \times 44.7\% \qquad (1)$$

where M_{Sb}, $M_{Co_2O_3}$ and $M_{Sb_2O_4}$ are the molar mass of Sb, Co_2O_3 and Sb_2O_4, respectively.

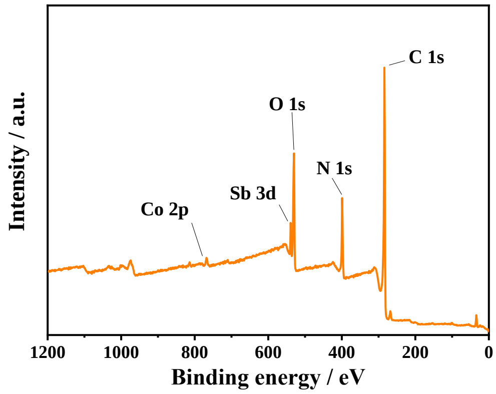

Figure S4. XPS survey spectrum of NC@CoSb/CNTs-400.

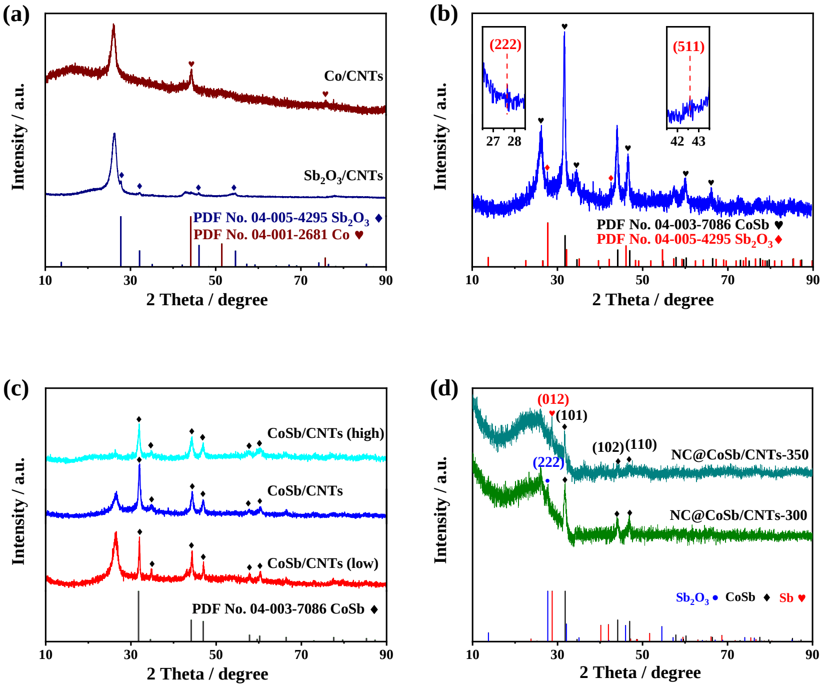

Figure S5. XRD patterns of (a) Sb_2O_3/CNTs and Co/CNTs, (b) CoSb/CNTs, (c) CoSb/CNTs, CoSb/CNTs(high) and CoSb/CNTs(low), (d) NC@CoSb/CNTs-300 and NC@CoSb/CNTs-350.

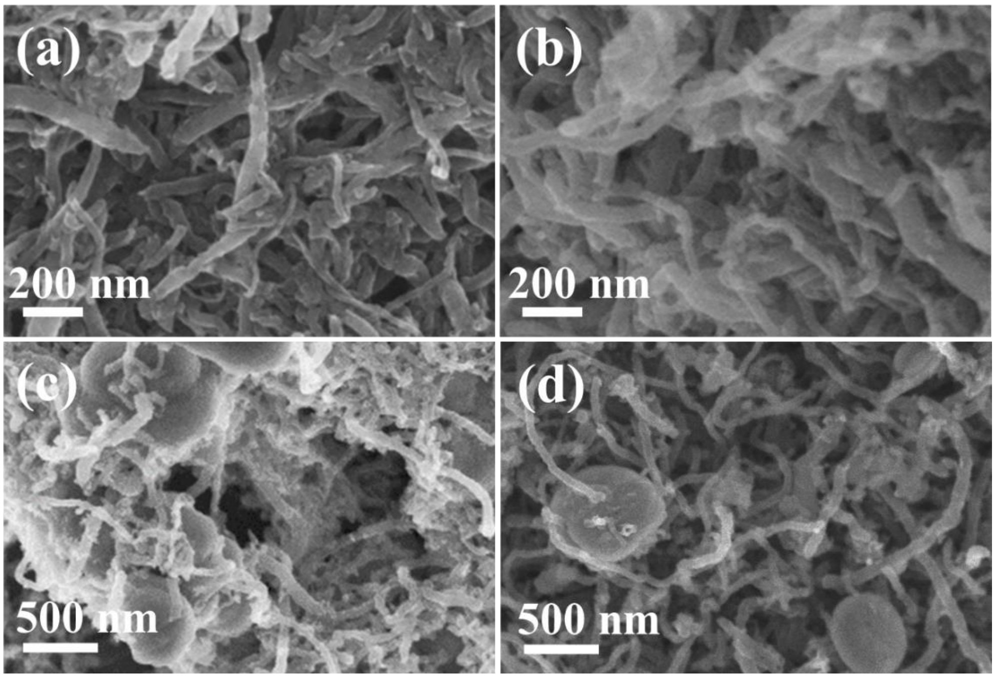

Figure S6. SEM images of (a) Sb_2O_3/CNTs, (b) Co/CNTs, (c) CoSb/CNTs (high) and (d) CoSb/CNTs-400.

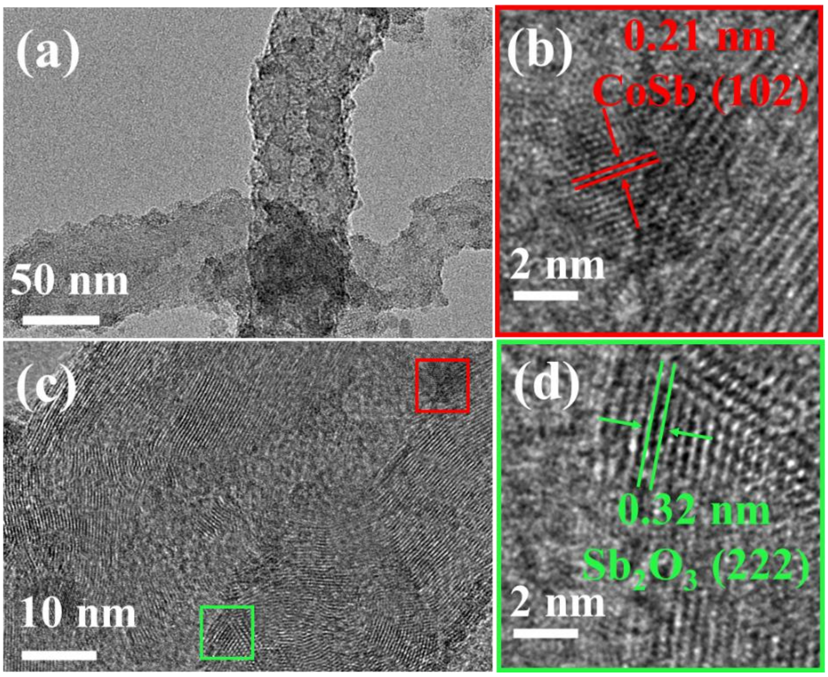

Figure S7. (a) TEM image and (c) HRTEM images of CoSb/CNTs. (b) and (d) magnified HRTEM images of CoSb/CNTs indicated in (c).

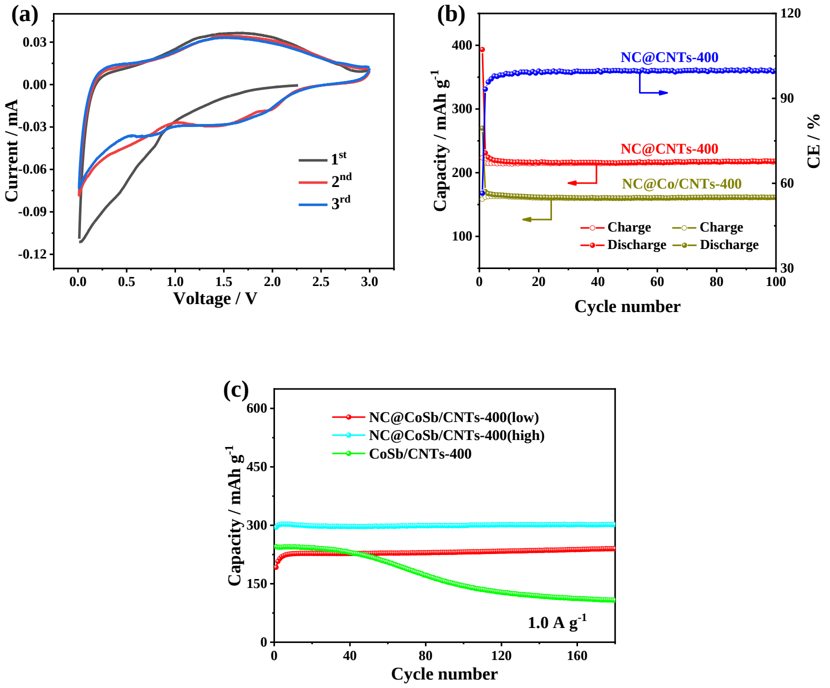

Figure S8. (a) CV curves of NC@CNTs-400. (b) Cycling performance of NC@CNTs-400 and NC@Co/CNTs-400 at 0.1 A g^{-1}. (c) Cycling performance of CoSb/CNTs-400, NC@CoSb/CNTs-400(low), and NC@CoSb/CNTs-400(high) at 1.0 A g^{-1}.

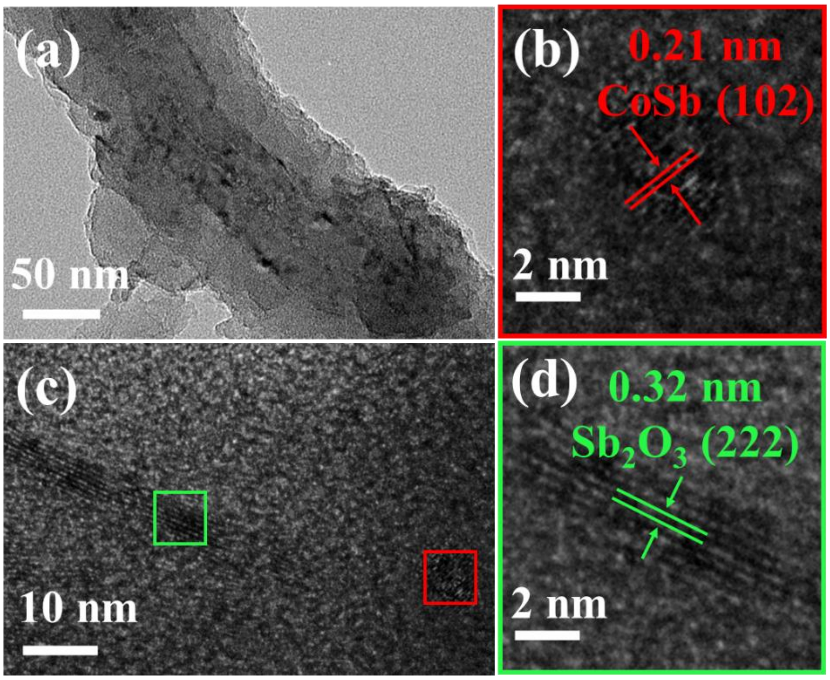

Figure S9. (a) TEM and (c) HRTEM images of NC@CoSb/CNTs-300. (b) and (d) magnified HRTEM images of CoSb/CNTs indicated in (c).

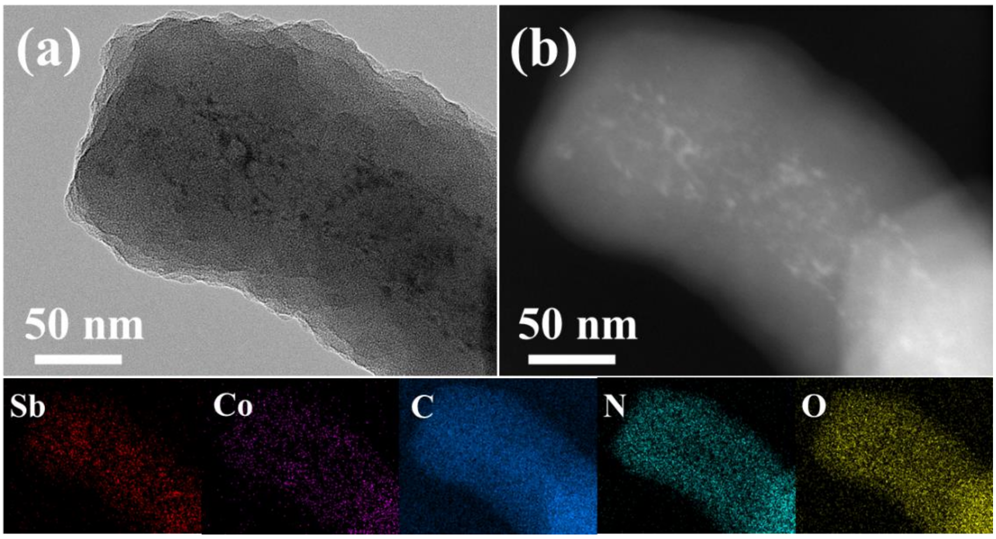

Figure S10. (a) TEM and (b) Elemental mapping images of the NC@CoSb/CNTs-400 after 500 cycles.

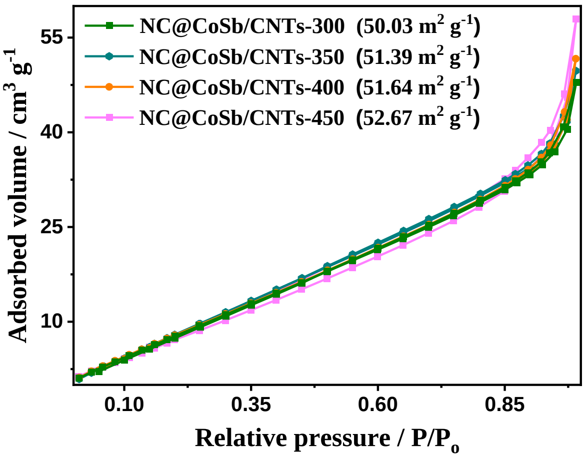

Figure S11. N_2 adsorption/desorption isotherms of NC@CoSb/CNTs-300, NC@CoSb/CNTs-350, NC@CoSb/CNTs-400 and NC@CoSb/CNTs-450. The BET specific surface areas of the samples are given in the brackets.

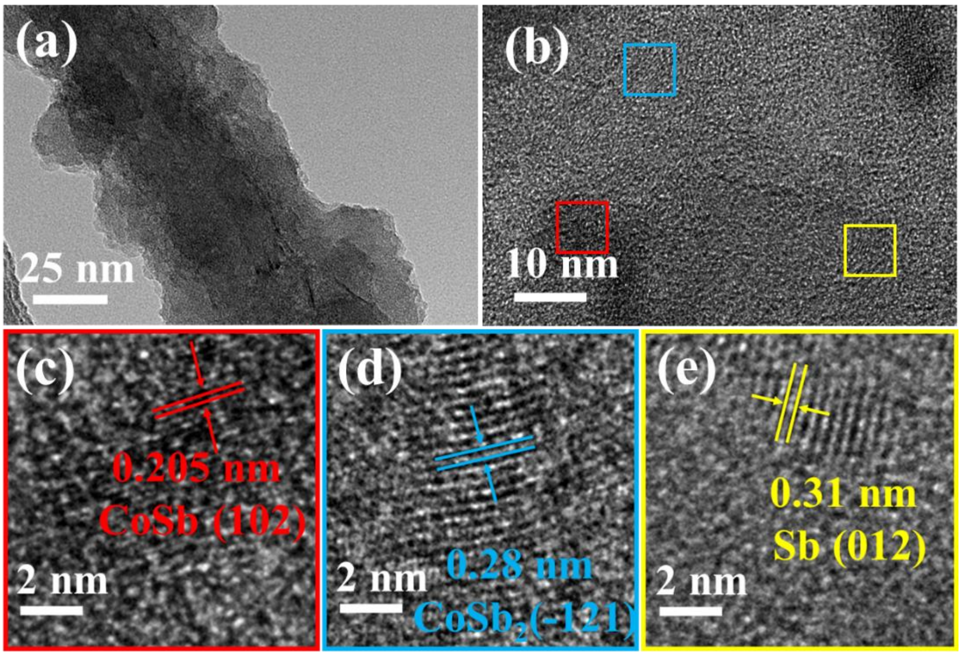

Figure S12. (a) TEM and (b) HRTEM images of NC@CoSb/CNTs-450. (c), (d) and (e) magnified HRTEM images of CoSb/CNTs indicated in (b).

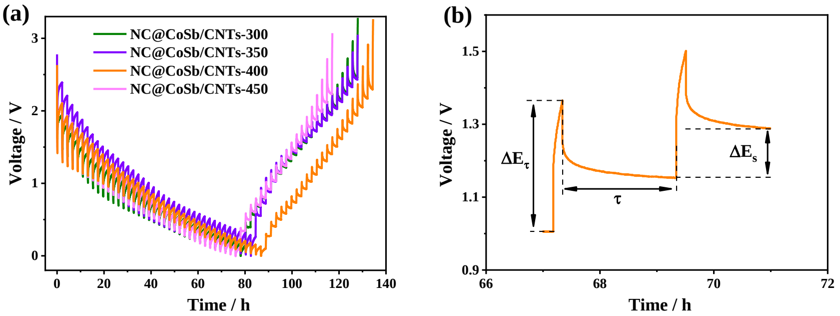

Figure S13. (a) GITT profiles of the discharge/charge process. (b) Schematic illustration of ΔE_s and ΔE_τ used for the calculation.

The diffusion coefficient is calculated using the following equation [3]:

$$D_{Na^+} = \frac{4}{\pi\tau}\left(\frac{mV_M}{M_wS}\right)^2\left(\frac{\Delta E_s}{\Delta E_\tau}\right)^2 \qquad (2)$$

where τ is the current pulse time (s), m is the mass of the active material, M_W is the molar mass of the active material, V_M is the molar volume of the active material, S is the geometric area of the electrode, and ΔE_s and ΔE_τ are defined as shown in **Figure S8**.

Table S1. Performance comparison of the NC@CoSb/CNTs with other Sb based anodes reported for the SIBs.

Material	Mass loading (mg cm^{-2})	Current density (A g^{-1})	Cycle number	Capacity (mAh g^{-1})	Capacity retention	Ref.
NC@CoSb/CNTs	1.0	1.0	1000	330.9	~100%	This work
		5.0	10000	261.2	92.1%	
		10.0	10000	255.9	88.5%	
3D Bi_3Sb_1/N-PC	1.0	10.0	6000	244.5	67.6%	4
c-Sb@a-TiPOx	1.0-1.5	1.0	1000	207.1	71%	5
		5.0	-	86.8	-	
Sb_2O_3@Sb@NC	0.6-0.8	10.0	10000	245.2	-	6
a-Sb/NC	1.5	1.0	500	280.5	80%	7
		2.0	-	298.7	-	
Bi–Sb/C	0.9	2.0	2500	233.2	71%	8
Sb@N,S-CNFs	-	2.0	1000	272	90.9%	9
		4.0	-	219	-	
Sb SQ@MA	1.0	1.0	1000	314	94%	10
		3.2	-	246		
peapod-like Sb@C	1.0-1.5	1.0	3000	305	70%	11
		10.0	-	206		
$Bi_{0.75}Sb_{0.25}$ array	-	0.5	2000	284	87%	12
Sb@Void@GDY	1.0	1.0	8000	325	74%	2
Sb/ACNTs-7	-	1.0	4500	318	48.4%	13
Sb@P-N/C	0.8-1.5	1.0	400	300	-	14
		5.0	400	249.9	90%	
Sb@C@TiO_2 TSNB	1.0	5.0	-	257	-	15
		10.0	-	212	-	
Sb@C	0.9	1.0	2000	230	56%	16
$(Bi_{0.47}Sb_{0.53})\ PO_4$/G	1.0	0.5	400	288	99%	17
Sb–N–C	0.6	1.0	2000	254	-	18
		10.0	-	155	-	
BiSb@C	1.0	1.0	600	284.7	97.5%	19
$SbVO_4$/rGO	1.0-1.5	1.0	2000	230	-	20
NiN-Sb_2Se_3@C	1.2-1.5	2.0	10000	135.2	-	21

References

1. B. Chen, Z. Jiang, J. Huang, B. Deng, L. Zhou, Z.-J. Jiang and M. Liu, *J. Mater. Chem. A*, 2018, **6**, 9517-9527.
2. Y. Liu, Y. Qing, B. Zhou, L. Wang, B. Pu, X. Zhou, Y. Wang, M. Zhang, J. Bai, Q. Tang and W. Yang, *ACS Nano*, 2023, **17**, 2431-2439.
3. Y. Xu, C. Zhang, M. Zhou, Q. Fu, C. Zhao, M. Wu and Y. Lei, *Nat. Commun.*, 2018, **9**, 1720.

4. X. Wang, B. Feng, L. Huang, Q. Fu, W. Li, C. Zhu, P. Chen, C. Yang and Y.-L. Ding, *J. Power Sources*, 2022, **520**, 0378-7753.
5. J. Pan, K. Yu, H. Mao, L. Li, Y. Zhang, Y. Li, P. J. Ferreira and J. Yang, *Chem. Eng. J.*, 2020, **380**, 122624.
6. A. Xu, C. Huang, G. Li, K. Zou, H. Sun, L. Fu, J. Ju, Y. Song, S. Wu, Z. Xu and Y. Yan, *J. Mater. Chem. A*, 2021, **9**, 12169-12178.
7. J. Yang, J. Li, T. Wang, P. H. L. Notten, H. Ma, Z. Liu, C. Wang and G. Wang, *Chem. Eng. J.*, 2021, **407**, 127169.
8. S. Guo, H. Li, Y. Lu, Z. Liu and X. Hu, *Energy Storage Mater.*, 2020, **27**, 270-278.
9. Z. Liu, H. Sun, X. Wang, Z.-Y. Gu, C. Xu, H. Li, G. Zhang, Y. He and X.-L. Wu, *Energy Storage Mater.*, 2022, **48**, 90-100.
10. X. Guo, H. Gao, S. Wang, G. Yang, X. Zhang, J. Zhang, H. Liu and G. Wang, *Nano Lett.*, 2022, **22**, 1225-1232.
11. K. Yang, J. Tang, Y. Liu, M. Kong, B. Zhou, Y. Shang and W. H. Zhang, *ACS Nano*, 2020, **14**, 5728-5737.
12. J. Ni, X. Li, M. Sun, Y. Yuan, T. Liu, L. Li and J. Lu, *ACS Nano*, 2020, **14**, 9117-9124.
13. C. Kang, S. Zhou, J. Liu, Y. Zhu, A. Hu, Q. Tang, Y. Zhang, X. Chen and T. Tao, *J. Mater. Chem. A*, 2021, **9**, 2152-2160.
14. N. Zhang, X. Chen, J. Xu, P. He and X. Ding, *ACS Appl. Mater. Interfaces*, 2023, **15**, 26728-26736.
15. M. Kong, Y. Liu, B. Zhou, K. Yang, J. Tang, P. Zhang and W. H. Zhang, *Small*, 2020, **16**, 2001976.
16. Z. Liu, X.-Y. Yu, X. W. Lou and U. Paik, *Energy Environ. Sci.*, 2016, **9**, 2314-2318.
17. Y. Yang, J. Wang, S. Liu, W. Zhu, G. Ye, X. Yi and B. Lu, *Chem. Eng. J.*, 2022, **435**, 134746.
18. Y. Tong, Y. Wu, X. Liu, Z. Chen and H. Li, *J. Colloid Interface Sci.*, 2023, **648**, 575-584.
19. P. Xiong, J. Wu, M. Zhou and Y. Xu, *ACS Nano*, 2020, **14**, 1018-1026.
20. J. Pan, Y. Zhang, L. Li, Z. Cheng, Y. Li, X. Yang, J. Yang and Y. Qian, *Small Methods*, 2019, **3**, 1900231.
21. Q. Li, W. Zhang, J. Peng, D. Yu, Z. Liang, W. Zhang, J. Wu, G. Wang, H. Li and S. Huang, *Adv. Funct. Mater.*, 2022, **32**, 2112776.